INTERNATIONAL JOURNAL OF ROBUST AND NONLINEAR CONTROL, VOL. 4, 301–319 (1994)

QUANTIFICATION OF MODEL UNCERTAINTY FROM DATA

DOUWE K. DE VRIES AND PAUL M. J. VAN DEN HOF

Mechanical Engineering, Systems and Control Group, Delft University of Technology, Mekelweg 2, 2628 CD Delft, The Netherlands

SUMMARY

Identification of linear models in view of robust control design requires the identification of a control-relevant nominal model, and a quantification of model uncertainty. In this paper a procedure is presented to quantify the model uncertainty of any prespecified nominal model, from a sequence of measurement data of input and output signals from a plant. By employing a nonparametric empirical transfer function estimate (ETFE), we are able to split the model uncertainty into three parts: the inherent uncertainty in the data due to data imperfections, the unmodelled dynamics in the nominal model, and the uncertainty due to interpolation. A frequency-dependent hard error bound is constructed, and results are given for tightening the bound through appropriate input design.

KEY WORDS Identification Frequency domain Model uncertainty Robust control

1. INTRODUCTION

In the systems and control community there is a growing interest in merging the problems of system identification and (robust) control system design. This interest is based on the conviction that, in many situations, models obtained from process experiments will be used as a basis for control system design. On the other hand, in model-based robust control design, models and model uncertainties have to be available that are essentially provided by, or at least validated by, measurement data from the process.

Recently several approaches to the identification problem have been presented, considering the identification in view of the control design. By far the most attention is paid to the construction of so-called hard error bounds, often referred to as H_∞-identification; see, for example, References 7, 8, 5, 10 and 15. In Reference 3 an identification procedure is presented that provides probabilistic (soft) error bounds.

In the references mentioned, there is a strong connection between the identification of nominal models and the quantification of model uncertainty. This has two serious drawbacks. Firstly, only identification methods for nominal models are selected for which (H_∞) error bounds can be derived. This seems to exclude many methods and model structures that could be useful but are rather intractable when it comes to deriving error bounds. When discussing the suitability of models as a basis for control system design, the availability of reliable hard error bounds certainly is important in order to obtain robust stability, and possibly also robust

This paper was recommended for publication by editor M. J. Grimble

CCC 1049–8923/94/020301–19

Received 22 April 1992
Revised 28 October 1992

performance. However, the nominal model that is used as a basis for the design will determine the nominal performance of the control system, and one will definitely not be willing to implement a control system when the nominal performance does not meet the specifications. As a result, the identification of nominal models, apart from the quantification of model uncertainty, is an important issue in identification for control design; see, for example, References 1, 2, 6, 13 and 14.

The second drawback is that one is not able to further tighten the error bound by doing additional experiments, without simultaneously changing the nominal model. For example, when the error bound is not tight enough and needs improvement in a specific frequency region, new experiments could be performed to reduce the uncertainty. However, when designing a new input signal it is not possible to restrict attention to the specific frequency region of interest, since this would essentially also affect the nominal model and the error bound outside this frequency region, and data sets from the different experiments cannot directly be combined to reduce the model uncertainty.

In addition to this reasoning, in this paper we will deal with the following problem: given a prespecified nominal model G_{nom} for an unknown linear plant G_0, can we construct an error bound for

$$|G_0(e^{j\omega}) - G_{\text{nom}}(e^{j\omega})| \tag{1}$$

based on noise corrupted measurements from input and output samples of the plant? Note that the nominal model may be available from any (control-relevant) identification procedure.

The problem is going to be tackled, through the construction of an intermediate data representation in the frequency domain, leading to the inequality:

$$|G_0(e^{j\omega_k}) - G_{\text{nom}}(e^{j\omega_k})| \leqslant |G_0(e^{j\omega_k}) - \hat{G}(e^{j\omega_k})| + |\hat{G}(e^{j\omega_k}) - G_{\text{nom}}(e^{j\omega_k})| \tag{2}$$

with $\hat{G}(e^{j\omega_k})$ an (intermediate) representation of the measurement data in the frequency domain. This means that $\hat{G}(e^{j\omega_k})$ basically is a finite number of complex points on the unit circle, obtained from the discrete Fourier transformation (DFT) of the time-domain data. The first term on the right-hand side of (2) can be considered to reflect inherent uncertainty in the data, whereas the second term is related to the quality of the nominal model, e.g. determined by unmodelled dynamics. Having constructed a data representation $\hat{G}(e^{j\omega_k})$, the second term can be calculated exactly. Hence, to give an upper bound on the model error $|G_0(e^{j\omega_k}) - G_{\text{nom}}(e^{j\omega_k})|$, the problem is to construct an upper bound for the error $|G_0(e^{j\omega_k}) - \hat{G}(e^{j\omega_k})|$. Note, however, that inequality (2) is only defined at the finite number of frequency points ω_k, while our aim is to bound the model error for all $\omega \in [0, 2\pi)$. The fact that the data does not contain information for frequencies $\omega \neq \omega_k$ gives rise to the uncertainty due to interpolation. The second problem therefore is to bound the model error for all $\omega \in [0, 2\pi)$ using the error bounds at ω_k. These two problems will be the main topics of this paper.

Related work has been published in References 10 and 8 where error bounds for $|G_0(e^{j\omega_k}) - \hat{G}(e^{j\omega_k})|$ have been obtained at a finite number of frequency points. In Reference 10 this has been done by employing the empirical transfer function estimate (ETFE, see Reference 11), and in Reference 8 through sinewave excitation and actually measuring the frequency response in a finite number of points. In References 5 and 7 the frequency-domain estimate and discrete error bound are used to obtain a model in H_∞ and a continuous error bound (valid on the whole unit circle). An attempt is made to keep the H_∞ error small by using an intermediate high order L_∞ model and Nehari approximation, obtaining a finite impulse response (FIR) model.

In Section 3 of this paper the ETFE is also used to obtain a nonparametric frequency-domain estimate $\hat{G}(e^{j\omega_k})$, and a discrete error bound. In contrast with References 5, 7 and 8, this error bound is frequency-dependent, which makes it more informative than a simple H_∞-bound. Moreover it does not require the frequency points of the discrete estimate to be equidistantly distributed over the unit circle. This paves the way for designing specific input signals in order to improve the estimates, and tightening the bound. Next a frequency-dependent continuous error bound is constructed in Section 4 by interpolation of the discrete bound, using smoothness properties of the system. In Section 5 it is shown how robust control design specifications can advocate new experiments in order to reduce the model uncertainty in specific frequency ranges. Finally, in Section 6, a simulation example is given to illustrate the merits of the procedure proposed.

2. PRELIMINARIES

It is assumed that the plant, and the measurement data that is obtained from this plant, allow a description

$$y(t) = G_0(q)u(t) + v(t) \tag{3}$$

with $y(t)$ the output signal, $u(t)$ the input signal, $v(t)$ an additive output noise, q^{-1} the delay operator, and G_0 a proper transfer function that is time-invariant and exponentially stable. The transfer function can be written in its Laurent expansion around $z = \infty$, as

$$G_0(z) = \sum_{k=0}^{\infty} g_0(k) z^{-k} \tag{4}$$

with $g_0(k)$ the impulse response of the plant. Throughout the paper we will consider discrete time intervals for input and output signals denoted by $T^N := [0, N-1]$, $T^N_{N_s} := [N_s, N+N_s-1]$ with N and N_s appropriate integers. We will denote

$$\sup_{t \in T^{N+N_s}} |u(t)| = \bar{u}$$

For a signal $x(t)$, defined on T^N, we will denote the N-point discrete Fourier transform (DFT) and its inverse by

$$X(2\pi k/N) = \sum_{t=0}^{N-1} x(t)\, e^{-j(2\pi k/N)t} \qquad \text{for} \qquad k \in T^N \tag{5}$$

$$x(t) = \frac{1}{N} \sum_{k=0}^{N-1} X(2\pi k/N)\, e^{j(2\pi k/N)t} \qquad \text{for} \qquad t \in T^N \tag{6}$$

When a signal $x(t)$ is defined on the interval $T^N_{N_s}$, $N_s > 0$, then we will denote the N-point DFT of a shifted version of the signal x, shifted over N_s time instants, by

$$X^s(2\pi k/N) = \sum_{t=0}^{N-1} x(t+N_s)\, e^{-j(2\pi k/N)t} \qquad \text{for} \qquad k \in T^N \tag{7}$$

$$x(t) = \frac{1}{N} \sum_{k=0}^{N-1} X^s(2\pi k/N)\, e^{j(2\pi k/N)(t-N_s)} \qquad \text{for} \qquad t \in T^N_{N_s} \tag{8}$$

Note that this reflects the N-point DFT of a signal, of which the first N_s time instants are discarded. Throughout this paper we will adopt a number of additional assumptions on the system and the generated data.

Assumption 2.1

There exists a finite

(i) $\bar{u}^p$, such that $|u(t)| \leqslant \bar{u}^p$ for $t < 0$;
(ii) pair of reals $\{M, \rho\} \in \mathbb{R}$, $\rho > 1$, such that $|g_0(k)| \leqslant M\rho^{-k}$, for $k \in \mathbb{Z}_+$;
(iii) upper bound on the DFT of the output noise: $|V^s(2\pi k/N)| \leqslant \bar{V}^s(2\pi k/N)$, for $k \in T^N$.

3. DISCRETE ERROR BOUND

3.1. Motivation

The motivation to consider the ETFE is that we want $\hat{G}(e^{j\omega_k})$ to be an intermediate data representation in the frequency domain. The ETFE is the quotient of the DFT of the output signal and the DFT of the input signal. In discrete Fourier transforming a signal no information is lost or added, the mapping from time to frequency domain is one to one. Also, the system is assumed to be linear. Therefore the ETFE can indeed be regarded as a representation of the data in the frequency domain.

The motivation to look at input design is that the ETFE for an arbitrary input signal is in general not satisfactory. We will try to improve the quality of the frequency domain data by input design.

3.2. Results

A nonparametric frequency-domain discrete upper bound on the additive error for the ETFE will be presented in this section. Errors due to unknown initial and final conditions of the system and additive noise on the output are taken into account. We will use a partly periodic input signal for excitation, and we will discard the first part of the signals in the estimation.

Definition 3.1

A partly periodic signal x is a signal having the first part equal to the last part: $x = [x_1 \; x_2 \; x_1]$.

The length of x_1 will be denoted by N_s. Only the part $[x_2 \; x_1]$ will be used in the identification and has length N. The total length of the signal x now is $N_s + N$. We will show that the value of N_s influences the error due to initial and final conditions in the estimate. Note that the largest possible value of N_s is N.

Theorem 3.2

Consider a SISO system, satisfying the assumptions stated in Section 2. Using a partly periodic input signal, $N_s \in T^{N+1}$, and the estimate

$$\hat{G}^s(2\pi l/N) = \frac{Y^s(2\pi l/N)}{U^s(2\pi l/N)} \qquad \text{for} \qquad l = \{l \in T^N \mid U^s(2\pi l/N) \neq 0\}$$

the following error bound is satisfied

$$| G_0(2\pi l/N) - \hat{G}^s(2\pi l/N) | \leqslant \alpha(2\pi l/N)$$

with

$$\alpha(2\pi l/N) = \frac{\bar{u}^p + \bar{u}}{| U^s(2\pi l/N) |} \frac{M\rho(1-\rho^{-N})}{(\rho-1)^2} \rho^{-N_s} + \frac{\bar{V}^s(2\pi l/N)}{| U^s(2\pi l/N) |}$$

Proof. See Appendix A. □

The first term on the right-hand side of the error bound given in the theorem is the error due to the effects of initial and final conditions of the system, i.e. the effects of the unknown signals outside the measurement interval. This error converges exponentially with N_s (convergence as ρ^{-N_s}). The properties of $| U^s(2\pi l/N) |$ of course depend on the specific choice of the input signal $u(t)$ for $t \in T^N_{N_s}$. For a random signal the expectation of the magnitude of the N-point DFT, as defined in (5) and (7), is asymptotically proportional to $\sqrt{N}$; see Reference 11, Lemma 6.2. Hence, if the input is random for $t \in T^N_{N_s}$, the error due to the effects of initial and final conditions converges approximately as $\rho^{-N_s}/\sqrt{N}$. The second term on the right-hand side is the error due to the additive noise on the output. This error does not converge at all, it is just the noise to signal ratio in the frequency domain. By designing an appropriate input signal, one can of course shape the error due to the noise. An input signal having a DFT with desired magnitude can be designed easily; see Reference 12.

We will now focus on the error due to the noise, the second term on the right-hand side of the error bound given in Theorem 3.2. It is possible to obtain convergence for this error by choosing the input signal to be periodic. The highest rate of convergence is obtained by an input signal having an integer number of periods in the interval $T^N_{N_s}$. Let N_0 denote the length of one period of the input signal and let the interval $T^N_{N_s}$ contain exactly k_0 periods, so that $N = k_0 N_0$. In this case $U^s(2\pi k/N) = 0$ if k/k_0 is not an integer, only $U^s(2\pi k/N_0)$ is not identically equal to zero, see Reference 11, Example 2.2. It is now straightforward to show that the DFT over k_0 periods of a periodic signal is exactly k_0 times as large as the DFT over one period. In conclusion, $| U^s(2\pi k/N_0) |$ is exactly proportional to N if $N = k_0 N_0$ with $k_0 \in \mathbb{Z}$.

Corollary 3.3

Consider a SISO system, satisfying the assumptions stated in Section 2. Using a partly periodic input signal having an integer number of periods in the interval $T^N_{N_s}$, $N_s \in T^{N+1}$, and the estimate

$$\hat{G}^s(2\pi l/N_0) = \frac{Y^s(2\pi l/N_0)}{U^s(2\pi l/N_0)} \qquad \text{for} \qquad l = \{l \in T^{N_0} \mid U^s(2\pi l/N_0) \neq 0\}$$

the following error bound is satisfied

$$| G_0(2\pi l/N_0) - \hat{G}^s(2\pi l/N_0) | \leqslant \alpha(2\pi l/N_0)$$

with

$$\alpha(2\pi l/N_0) = \frac{\bar{u}^p + \bar{u}}{| U^s(2\pi l/N_0) |} \frac{M\rho(1-\rho^{-N})}{(\rho-1)^2} \rho^{-N_s} + \frac{\bar{V}^s(2\pi l/N_0)}{| U^s(2\pi l/N_0) |}$$

The error bound given in the corollary goes to zero if N_s and N are going to infinity, N_0 is constant, and the noise $v(t)$ does not contain a periodic component. The error due to the

effects of initial and final conditions converges as ρ^{-N_s}/N. The error due to the additive noise on the output converges approximately as $1/\sqrt{N}$ if $v(t)$ is a random signal, because the expectation of the magnitude of the N-point DFT of a random signal is asymptotically proportional to $\sqrt{N}$, see Reference 11, Lemma 6.2, while the magnitude of the DFT of the periodic input is exactly proportional to N. The price for this convergence is that less points of the transfer function are estimated (N_0 instead of $N = k_0 N_0$).

3.3. Remarks

A partly periodic signal can be seen as a generalization of a sinewave input. This generalization is useful because sinewave testing (sinewave excitation and actually measuring the frequency response in a finite number of frequency points) is time-consuming. For each new sinewave input one must wait until the system has reached its steady-state response. A partly periodic signal can consist of N sinewaves, but one has to wait only one time for the effects of initial and final conditions to vanish.

For $N_s = 0$ the ETFE as defined in Reference 11 arises. In this case the error due to initial and final conditions converges as $1/\sqrt{N}$ if $u(t)$ is a random signal for $t \in T^N$, as was also shown in Reference 11. Note that for $N_s = 0$ the input signal is completely free. The choice for $N_s > 0$ hence is a choice to restrict the input signal in order to be able to obtain a tight error bound for the nominal model.

Finally we note that the extension to the MIMO case of Theorem 3.2 has been made by the authors. To do this, the Fourier transforms of the different input signals have to satisfy an orthogonality condition.

4. CONTINUOUS ERROR BOUND

4.1. Motivation

We now have an upper bound $\alpha(\omega_k)$ on the error $|G_0(e^{j\omega_k}) - \hat{G}(e^{j\omega_k})|$. This error bound is only defined in a finite number of frequency points $\omega_k \in \Omega$, with $\Omega := \{\omega_k \in \mathbb{R} \cap [0, 2\pi) \mid |U^s(e^{j\omega_k})| \neq 0\}$. This is due to the fact that $\hat{G}(e^{j\omega_k})$ is only defined at a finite number of frequency points when N, the number of data points used in the estimate, is finite. The aim is to find an upper bound $\delta(\omega)$ such that

$$|G_0(e^{j\omega}) - G_{\text{nom}}(e^{j\omega})| \leqslant \delta(\omega)$$

for all frequencies in the interval $[0, 2\pi)$. It is straightforward to give a discrete upper bound $\delta(\omega_k)$. First note that $\beta(\omega_k) = |\hat{G}(e^{j\omega_k}) - G_{\text{nom}}(e^{j\omega_k})|$ can be calculated exactly because G_{nom} is assumed to be known. From the inequality

$$|G_0(e^{j\omega_k}) - G_{\text{nom}}(e^{j\omega_k})| \leqslant |G_0(e^{j\omega_k}) - \hat{G}(e^{j\omega_k})| + |\hat{G}(e^{j\omega_k}) - G_{\text{nom}}(e^{j\omega_k})| \tag{9}$$

it now follows that a possible choice for $\delta(\omega_k)$ is $\delta(\omega_k) = \alpha(\omega_k) + \beta(\omega_k)$. Hence the problem is to find the behaviour of $\delta(\omega)$ between the estimated frequency points for the prespecified nominal model. As argued in Section 3.1, the data does not essentially contain more information about the transfer function of the system than is captured by the discrete estimate $\hat{G}(e^{j\omega_k})$. Therefore, assumptions about the system must be used to be able to bound the error at frequencies $\omega \neq \omega_k$. We will use smoothness assumptions on the system, and we will interpolate the discrete error bound $\delta(\omega_k)$ using these smoothness properties.

Note that we will not interpolate $\alpha(\omega_k)$, as is done in Reference 7. To be able to interpolate $\alpha(\omega_k)$, one first has to interpolate the discrete estimate $\hat{G}(e^{j\omega_k})$. However, in doing this, an intermediate model is constructed that is not based on the data. Therefore we take the approach of interpolating the error bound $\delta(\omega_k)$.

4.2. Bounds on derivatives

Smoothness properties of the system in the form of upper bounds on the derivatives of $G_0(e^{j\omega})$ with respect to frequency, can be obtained from the assumed upper bound on the impulse response.

Proposition 4.1

For a SISO system with $|g_0(m)| \leqslant M\rho^{-m}$ there holds

$$\left|\frac{dG_0(e^{j\omega})}{d\omega}\right| = \frac{M\rho}{(\rho-1)^2}$$

$$\left|\frac{d^2G_0(e^{j\omega})}{d\omega^2}\right| \leqslant \frac{M\rho(\rho+1)}{(\rho-1)^3}$$

Proof. See Appendix B. □

The SISO system is allowed to be an element of a MIMO system. In that case G_0 must be replaced by $G_{0[ij]}$, g_0 by $g_{0[ij]}$, M by $M_{[ij]}$ and ρ by $\rho_{[ij]}$.

Note that the upper bounds on the derivatives are not obtained in the same way as in Reference 7, the M and ρ used in this paper are different from the ones used there. It is the authors' opinion that it is easier in practice to obtain a good upper bound on the impulse response, than to obtain a margin of relative stability of the system together with the infinity norm of the system over the circle in the complex plane with radius equal to this margin as used in Reference 7.

To be able to bound the derivatives of the magnitude of the error system $|G_0(e^{j\omega}) - G_{\text{nom}}(e^{j\omega})|$ we need the following proposition.

Proposition 4.2

For a SISO system there holds

$$\left|\frac{d^k}{d\omega^k}\,|G_0(e^{j\omega}) - G_{\text{nom}}(e^{j\omega})|\right| \leqslant \left|\frac{d^k}{d\omega^k}\,(G_0(e^{j\omega}) - G_{\text{nom}}(e^{j\omega}))\right| \tag{10}$$

$$\leqslant \left|\frac{d^kG_0(e^{j\omega})}{d\omega^k}\right| + \left|\frac{d^kG_{\text{nom}}(e^{j\omega})}{d\omega^k}\right| \tag{11}$$

for $k = 1$ and $k = 2$.

Proof. See Appendix C. □

Again, the SISO system is allowed to be an element of a MIMO system.

An upper bound for (11) can be calculated using Proposition 4.1 and the knowledge of $G_{\text{nom}}(e^{j\omega})$. If an upper bound on $|g_0(m) - g_{\text{nom}}(m)|$ is known, we are able to calculate an upper bound for (10) directly from Proposition 4.1.

4.3. Interpolation

In this section we will address the problem of calculating an upper bound on the error $|G_0(e^{j\omega}) - G_{nom}(e^{j\omega})|$ between the frequency points ω_k where an upper bound $\delta(\omega_k)$ is known. Hence, we have to find the highest possible value $\delta(\omega)$ of this error for each frequency ω between two given points, say $\delta(\omega_k)$ and $\delta(\omega_{k+1})$. We are able to bound this error by taking into account the bounds on the first and second derivatives of $|G_0(e^{j\omega}) - G_{nom}(e^{j\omega})|$ that were derived in Section 4.1, say γ_1 and γ_2 respectively. The maximum value of the error $\delta(\omega)$ now arises by interpolating the discrete error bound $\delta(\omega_k)$ using the function $f(x)$ depicted in Figure 1. To explain the construction of this function $f(x)$, assume that there is a maximum between the two frequency points. Starting at the maximum ($x = 0$, $f(x) = 0$ and $df(x)/dx = 0$) we want $f(x)$, in a smooth way, to decrease as fast as possible: the faster $f(x)$ decreases, the higher the maximum lies above the two given points $\delta(\omega_k)$, $\delta(\omega_{k+1})$. Hence we use a function having a constant second derivative equal to the bound γ_2 on this derivative. In this way parts II and III of the error bound are constructed. The absolute value of the first derivative of this function will clearly increase with the distance $|x|$ to the maximum. At $|x| = \gamma_1/\gamma_2$ the first derivative becomes equal to the bound γ_1 on this derivative. Hence, for $|x| > \gamma_1/\gamma_2$ we use a function having a constant first derivative equal to the bound γ_1. In this way part I or IV of the error bound is constructed. The function constructed in this way is unique and given by

$$\begin{aligned} f(x) &= -\frac{\gamma_2}{2}x^2 && \text{for} \quad |x| \leqslant \frac{\gamma_1}{\gamma_2} \\ &= -\gamma_1|x| + \frac{\gamma_1^2}{2\gamma_2} && \text{for} \quad |x| > \frac{\gamma_1}{\gamma_2} \end{aligned} \tag{12}$$

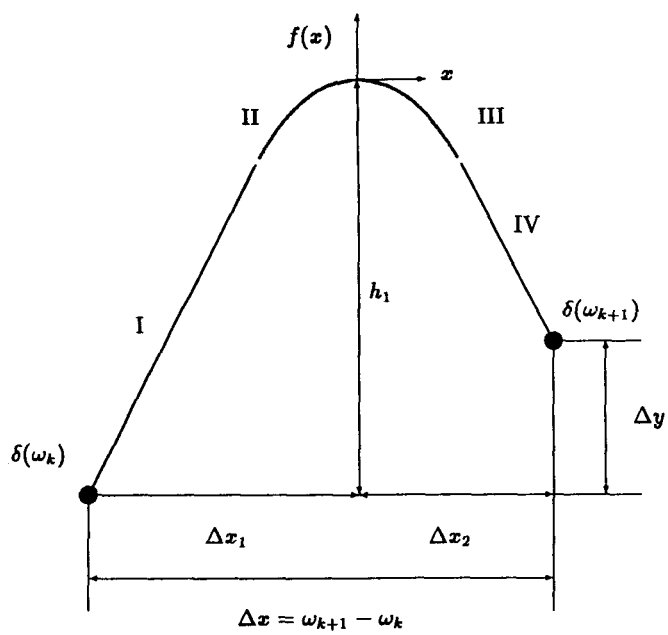

Figure 1. The interpolating function $f(x)$ for the discrete error bound

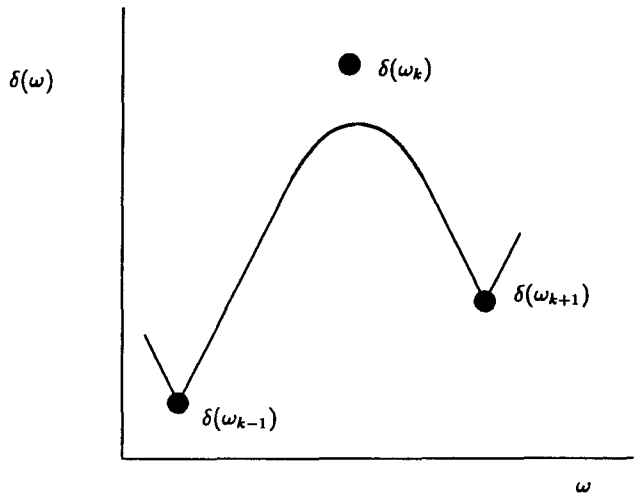

Figure 2. A situation in which the point $\delta(\omega_k)$ must not be used

The function $f(x)$ given in (12) directly gives the value of $\delta(\omega)$

$$\delta(\omega) = \delta(\omega_k) - f(\Delta x_1) + f(x) \qquad \text{for} \qquad \omega \in [\omega_k, \omega_{k+1}] \tag{13}$$

However, in (13) the values of Δx_1 and x are unknown, because the location of the maximum is as yet unknown. Analytic expressions for the location of the maximum can be given, by specifying Δx_1 or Δx_2 as a function of $\delta(\omega_k)$, $\delta(\omega_{k+1})$, γ_1 and γ_2. These expressions are given in Algorithm D.1, see Appendix D. Using this algorithm we are able to give an upper bound for the difference between the system and the nominal model for all $\omega \in [0, 2\pi)$.

When $|\Delta y| > \gamma_1 \Delta x$ the estimated point of the discrete estimate with the highest error bound must not be used. Interpolation from neighbouring points, although over a greater distance, gives a lower error bound. This situation can also arise when $|\Delta y| \leqslant \gamma_1 \Delta x$; see Figure 2.

Note that, as opposed to References 7 and 5, Algorithm D.1 allows for a discrete error bound that is frequency-dependent, and it yields a continuous error bound that is frequency-dependent. Moreover the discrete frequency points are not required to be equidistant.

4.4. Remarks

Taking a closer look at the results of this and the previous section, we can summarize in the following way. In Section 3 a bound $\alpha(\omega_k)$ has been derived

$$|G_0(e^{j\omega_k}) - \hat{G}(e^{j\omega_k})| \leqslant \alpha(\omega_k) \tag{14}$$

for all ω_k in a set $\Omega \subset \mathbb{R} \cap [0, 2\pi)$ containing a finite number ($\leqslant N$) of elements. Since the nominal model is known, the error

$$\beta(\omega_k) := |\hat{G}(e^{j\omega_k}) - G_{\text{nom}}(e^{j\omega_k})| \tag{15}$$

can be calculated exactly for all $\omega_k \in \Omega$. In this Section 4, a continuous bound $\delta(\omega)$ is derived, such that

$$|G_0(e^{j\omega}) - G_{\text{nom}}(e^{j\omega})| \leqslant \delta(\omega) \tag{16}$$

with

$$\delta(\omega_k) = \alpha(\omega_k) + \beta(\omega_k) \qquad \text{for} \qquad \omega_k \in \Omega \tag{17}$$

In the nonparametric discrete estimate, cf. (14), no error due to under-modelling is present, i.e. no error due to approximation is made, because complete freedom exists for each frequency point to fit $G_0(e^{j\omega_k})$. The approximation error therefore is completely due to the nominal model, cf. (15).

In the procedure presented, the determination of the nominal model and the determination of the error bound clearly are completely separated. We addressed the problem of determining the error bound. The problem of determining, from the discrete estimate, a nominal model such that the error bound is as low as possible is addressed in References 7 and 5. Methods for tuning the nominal model to nominal control design specifications are discussed in References 2, 6, 13 and 14.

The procedure presented can very well be used to obtain an upper bound on the unmodelled dynamics, as is needed in References 15 and 9.

5. RELATION WITH CONTROL DESIGN SPECIFICATIONS

To show the applicability of the approach presented in this paper to robust control design, we will consider the following situation. In order to verify desired robustness properties of a designed controller for the system, an allowable error bound is specified for the difference between G_0 and G_{nom}:

$$|G_0(e^{j\omega}) - G_{\text{nom}}(e^{j\omega})| \leqslant \delta_a(\omega)$$

The allowable error $\delta_a(\omega)$ is a function of the nominal model, the designed controller and the robust control design specifications. Given measurement data from the system, it now has to be verified whether a specific nominal model lies within the specified error bound. If not, it should be determined which action should be taken in order to solve the problem: either constructing a new nominal model, or performing additional experiments to reduce the uncertainty.

The actual error bound $\delta(\omega)$ for the nominal model clearly is a function of the nominal model itself and of the discrete estimate $\hat{G}$. Therefore both should be tuned to the robust control design specifications. This can be done by comparing the allowable error $\delta_a(\omega)$ with the actual error bound $\delta(\omega)$. For those values of ω where $\delta(\omega) > \delta_a(\omega)$ we can analyse $\delta(\omega)$ and evaluate its different components.

At the finite number of frequency points $\omega_k \in \Omega$, we have $\delta(\omega_k) = \alpha(\omega_k) + \beta(\omega_k)$. Therefore we know that

(1) when $\alpha(\omega_k) \gg \beta(\omega_k)$, the uncertainty is mainly due to the inherent uncertainty in the data $\alpha(\omega_k)$, i.e. effects of initial and final conditions, bad signal-to-noise ratio and/or restricted length of the data set. Actions to be taken to improve the bound include: increasing N_s, increasing the power of the input signal, and increasing N. In the case of periodic input signals, the signal-to-noise ratio in the frequency domain is proportional to $\sqrt{N/N_0}$. Consequently the error bound can also be improved by decreasing N_0;

(2) when $\alpha(\omega_k) \ll \beta(\omega_k)$, the uncertainty is mainly due to a bad nominal model. A straightforward action is then to choose a new nominal model that is better able to represent the system dynamics in the specific frequency range.

In between the finite number of frequency points $\omega_k \in \Omega$, say for $\omega_k < \omega < \omega_{k+1}$, the error

bound $\delta(\omega)$ is determined through interpolation between the adjacent points $\delta(\omega_k), \delta(\omega_{k+1})$. Therefore

3. when $\delta(\omega) \gg \max(\delta(\omega_k), \delta(\omega_{k+1}))$, the uncertainty is mainly due to the interpolation step. Note that uncertainty due to interpolation is strongly determined by the distance between two adjacent discrete frequency points. Consequently new experiments should be performed with a smaller distance between the discrete frequency points in the specific frequency region.

Note that it is possible to determine whether the main source of the actual error is the inherent uncertainty in the data, the nominal model, or the interpolation step caused by the absence of data due to the specific excitation of the system. Also it is possible to decrease the contribution of these different error sources almost independently. Now it is possible to iteratively decrease the error bound, until the level of the allowable error is reached, successively by input design and additional experiments, and by tuning the nominal model. Using this procedure we can determine whether or not specific robust control design specifications can be met.

Both the inherent uncertainty in the data $\alpha(\omega_k)$, and the error due to interpolation can be made arbitrarily small, *casu quo* the error bound can be made arbitrarily tight, in a certain frequency region by improving the discrete estimate. Note that the error bound $\alpha(\omega_k)$ is essentially frequency-dependent and that the frequency points $\omega_k \in \Omega$ need not be positioned equidistantly over the frequency axis. In comparison with References 7 and 5, this creates a lot of freedom to shape the error bound into an accepted (allowable) form, which — from a control point of view — definitely should be frequency-dependent.

6. EXAMPLE

To illustrate our results a simulation was made of a fifth-order system

$$G_0(z) = \frac{0{\cdot}82 - 1{\cdot}04z^{-1} + 0{\cdot}28z^{-2} + 0{\cdot}61z^{-3} - 1{\cdot}05z^{-4} + 0{\cdot}47z^{-5}}{1 - 2{\cdot}47z^{-1} + 2{\cdot}88z^{-2} - 1{\cdot}97z^{-3} + 0{\cdot}81z^{-4} - 0{\cdot}17z^{-5}}$$

whose impulse response satisfies a bound given by $M_0 = 3$ and $\rho_0 = 1{\cdot}256$. There was 10 percent (in amplitude) coloured noise (high-pass-filtered white noise) on the output. The nominal model is given as

$$G_{\text{nom}}(z) = \frac{0{\cdot}79 + 0{\cdot}09z^{-1} - 0{\cdot}24z^{-2} + 0{\cdot}63z^{-3}}{1 - 1{\cdot}25z^{-1} + 0{\cdot}75z^{-2} + 0{\cdot}05z^{-3}}$$

Based on this nominal model a robust controller was designed for the system

$$C_0(z) = \frac{1{\cdot}60z^{-2} - 1{\cdot}18z^{-3} + 0{\cdot}81z^{-4}}{1 - 2{\cdot}85z^{-1} + 3{\cdot}45z^{-2} - 2{\cdot}28z^{-3} + 0{\cdot}69z^{-4}}$$

In this example we will focus on the following two questions

- When the controller is applied to the true system $G_0(z)$, will the resulting closed loop configuration be stable?
- What is the quality of the nominal model?

To answer the first question we will investigate whether the loop gain $G_0(\omega)C_0(\omega)$ does encircle the point -1 in the Nyquist diagram. In order to build in some safety, *casu quo* some robust performance, we require in addition that the loop gain does not enter a circle with radius $0{\cdot}3$

around the point -1. The resulting allowable uncertainty is

$$\delta_a(\omega) = \frac{|\, G_{nom}(\omega)C_0(\omega) + 1\,| - 0{\cdot}3}{|\, C_0(\omega)\,|}$$

As *a priori* information on the impulse response we choose $M = 3$ and $\rho = 1{\cdot}2$. The upper bound $\bar{V}^s(\omega_k)$ was set to $\bar{V}^s(\omega_k) = 3\sqrt{\Phi_v(\omega_k)N}$, where $\Phi_v(\omega_k)$ denotes the spectrum of the noise. For normally distributed noise this upper bound has a probability of 99·99 per cent of being valid, and indeed was satisfied for all experiments.

The input signal was chosen to obey $\bar{u}^p = 2$ and $\bar{u} = 1$. For the first experiment we used 178 points with $N = 128$, $N_0 = 128$ and $N_s = 50$. The magnitude of the DFT of the input signal in the interval $T^N_{N_s}$, $|\, U^s(\omega_k)\,|$, is given in Figure 3. In Figure 4 the allowable error $\delta_a(\omega)$, the error bound $\delta(\omega)$ and the error due to approximation $\beta(\omega_k)$ are given. The inherent uncertainty in the data $\alpha(\omega_k)$ equals $\delta(\omega_k) - \beta(\omega_k)$. The error due to interpolation is indicated by the curves between the points $\delta(\omega_k)$. Clearly, in the frequency interval $\omega = [0{\cdot}8, 1{\cdot}3]$ rad/s it is possible that the actual error is larger than the allowable one, so that no stability guarantee can be given.

In order to be able to improve the error bound we will take a closer look at the error-generating processes. The true error due to approximation is fixed, because the nominal model is fixed. Using the prior information M, ρ, $\bar{u}^p$ and $\bar{u}$, it follows from Corollary 3.3 that the error due to initial and final conditions is less than 0·01, and therefore is neglectable. Hence we can only improve upon the errors due to noise and interpolation. From Figure 4 it follows that in the frequency interval $\omega = [0{\cdot}8, 1{\cdot}1]$ rad/s the noise as well as the interpolation error needs to be improved. In the frequency interval $\omega = [1{\cdot}1, 1{\cdot}3]$ rad/s it probably will suffice to decrease the error due to the noise only.

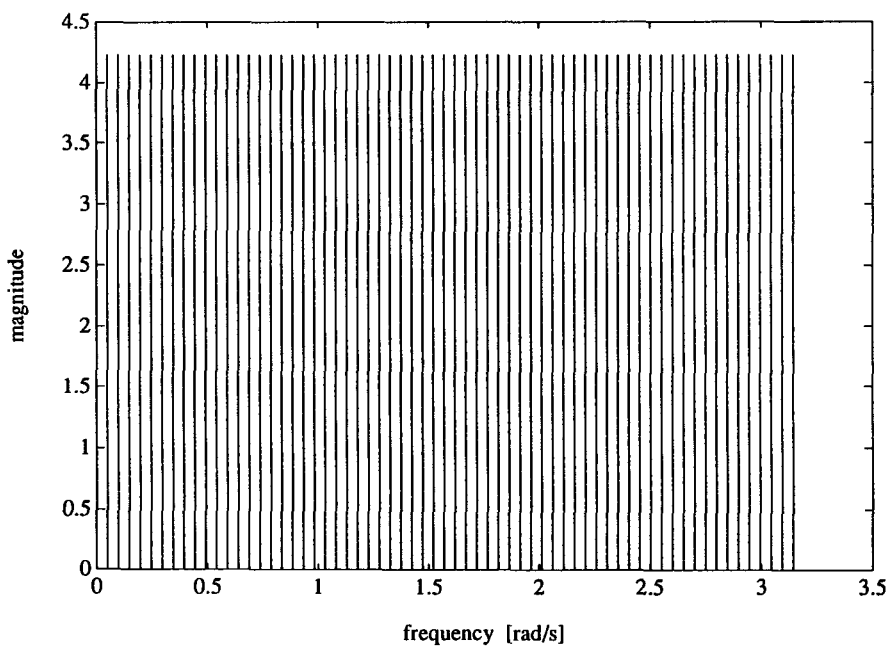

Figure 3. $|\, U^s(\omega_k)\,|$, the magnitude of the DFT of the input signal in the interval $T^N_{N_s}$

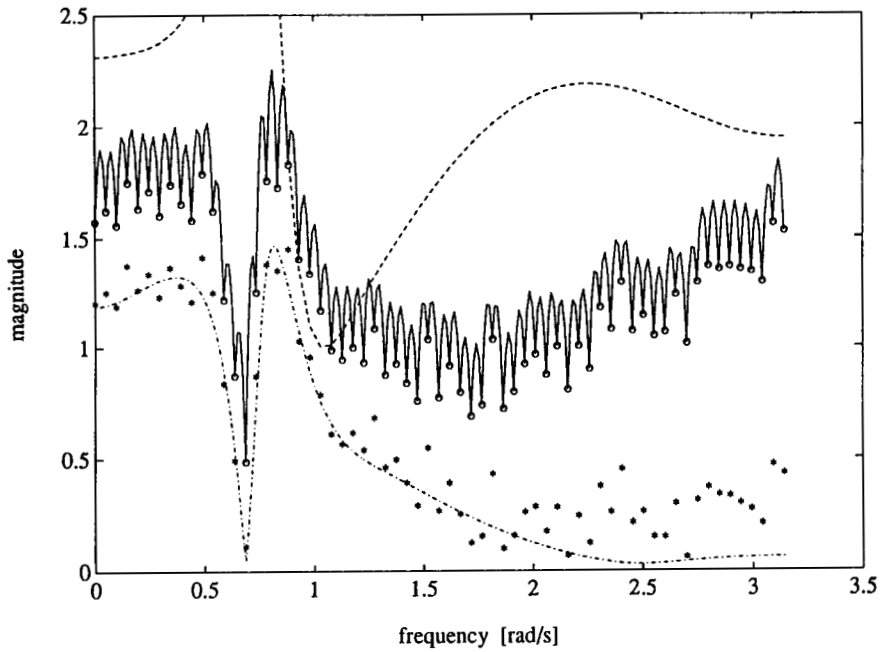

Figure 4. The error bounds and the true error: $\delta_a(\omega)$ (dashed line), $\delta(\omega)$ (solid line), $\delta(\omega_k)$ (○), $\beta(\omega_k)$ (*), $|G_0(\omega) - G_{nom}(\omega)|$ (chain line)

The specific improvements mentioned above can be achieved accurately by input design. The magnitude of the DFT of the new input signal is given in Figure 5. We choose $N = 512$, $N_0 = 256$ and $N_s = 50$. We used an input signal having two periods, in order to obtain a higher signal to noise ratio in the frequency domain $|U^s(\omega_k)|/|V^s(\omega_k)|$ compared to the previous experiment, while maintaining the constraint $\bar{u} = 1$. Also, the period length N_0 was increased to obtain a denser DFT frequency grid. This denser grid is needed in the frequency interval $\omega = [0{\cdot}8, 1{\cdot}1]$ rad/s to be able to reduce the distance between two frequency points ω_k when compared to Figure 3, in order to decrease the error due to interpolation in this frequency region. The magnitude of the DFT of the input signal was shaped as follows. Because the error due to initial and final conditions is neglectable, we have $\alpha(\omega_k) \approx \bar{V}^s(\omega_k)/|U^s(\omega_k)|$. Also $\delta(\omega_k) = \alpha(\omega_k) + \beta(\omega_k) \leqslant 2\alpha(\omega_k) + |G_0(\omega_k) - G_{nom}(\omega_k)|$. Choosing $|U^s(\omega_k)| = 2(\delta_a(\omega_k) - |G_0(\omega_k) - G_{nom}(\omega_k)|)^{-1}\bar{V}^s(\omega_k)$ therefore would result in $\delta(\omega_k) \leqslant \delta_a(\omega_k)$. However, because G_0 is unknown, we choose $|U^s(\omega_k)|$ to be proportional to $(\delta_a(\omega_k) - \beta(\omega_k))^{-1}\bar{V}^s(\omega_k)$.

In Figure 6 the resulting error bounds are given, together with the allowable error and the true error. Note that $\beta(\omega_k)$ provides a good indication of the true error, and that the error bound $\delta(\omega)$ can be made almost equal to the true error by input design.

Combining the two error bounds, which is possible because the nominal model is fixed, proves that the actual error is indeed lower than the allowable error, meaning that the true closed loop system will be stable. The controller therefore can be implemented safely. However, the nominal model is not correct. A better nominal model certainly is desirable. If the control requirements would have been slightly more severe, a better (higher order) nominal model even would have been necessary to be able to prove stability of the closed loop. Clearly, the modelling error in the frequency interval $\omega = [0{\cdot}8, 1{\cdot}1]$ rad/s is crucial. A shorter

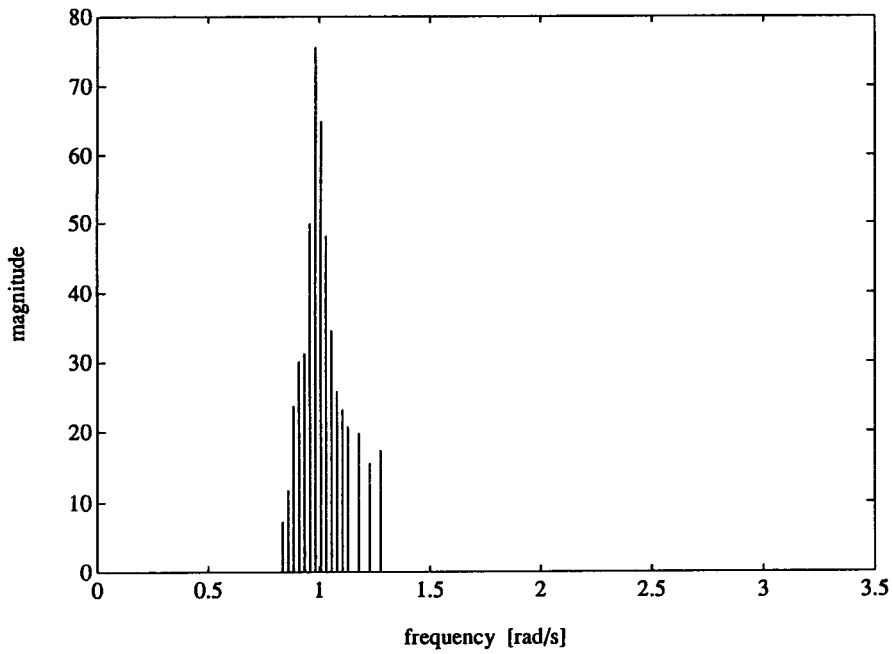

Figure 5. $|U^s(\omega_k)|$, the magnitude of the DFT of the input signal in the interval T_N^N,

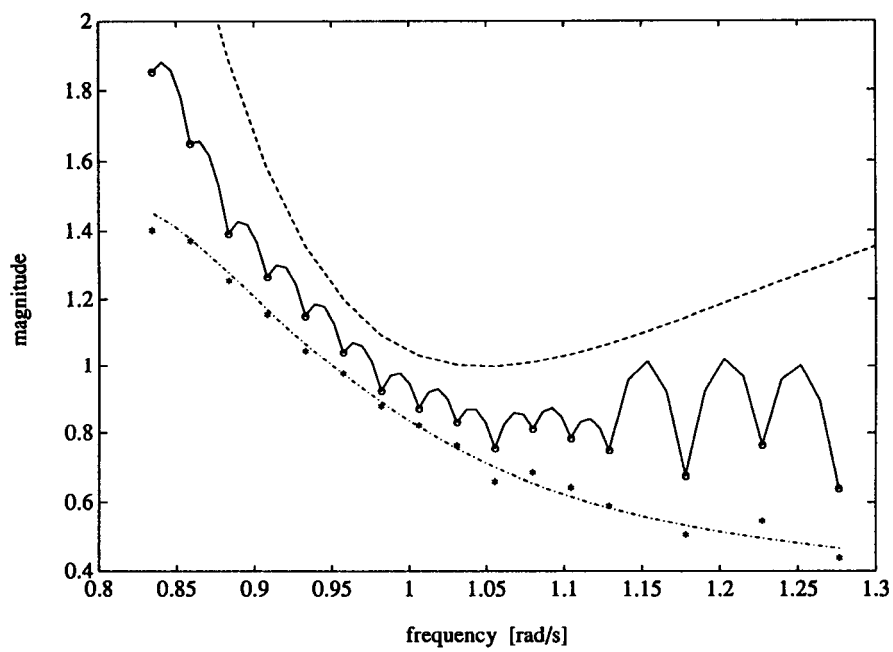

Figure 6. The error bounds and the true error: $\delta_a(\omega)$ (dashed line), $\delta(\omega)$ (solid line), $\delta(\omega_k)$ (○), $\beta(\omega_k)$ (*), $|G_0(\omega) - G_{\text{nom}}(\omega)|$ (chain line)

experimentation time would have been sufficient if the nominal model had been more accurate in this frequency interval.

The above demonstrates the interplay between the accuracy of the error bound (experimentation time), modelling accuracy (modelling effort, model order), and control specifications (robustness, performance).

7. CONCLUSIONS

In this paper a procedure is presented to quantify the model uncertainty of any prespecified nominal model, given a sequence of measurement data from a plant. In the procedure presented the empirical transfer function estimate (ETFE) is used to construct a (nonparametric) estimate of the transfer function in a finite number of frequency points, together with an upper bound on the error. Through interpolation, this error bound can be transformed to a bound which is available on a continuous frequency interval. A frequency-dependent upper bound is obtained, which is much more tailored to the needs of a robust control design scheme than an H_∞-bound. In order to obtain a tight error bound, a special input signal is proposed (partly periodic) which has advantages over (classical) sinewave experiments.

The estimated upper bound for the model error of a prespecified nominal model can be split into three parts: one part due to the inherent uncertainty in the data, a second part due to interpolation, and a third part due to imperfections of the nominal model. These three components can be tuned almost independently, by appropriate experiment design and by choosing an appropriate nominal model. When the error bound is too conservative in relation with control design specifications, information is provided as to which action should be taken (new experiments or alternative nominal model) in order to satisfy the design requirements. Because the nominal model is not a fixed function of the data, it is not necessary to change the nominal model when a new set of measurements is used. Therefore it is possible to restrict attention to a specific frequency region when designing the new input signal, the error bound for other frequencies remains valid if the nominal model is not changed.

APPENDIX A: PROOF OF THEOREM 3.2

A.1. Properties of the N-point DFT

To give the proof we have to start by taking a closer look at the properties of the N-point DFT, and by dealing with some additional definitions and notation. The periodic continuation of a signal $x(t)$ is denoted by $x^{\mathrm{R}}(t)$

$$x^{\mathrm{R}}(t+kN) = x(t) \qquad \text{for } k \in \mathbb{Z},\ t \in T^N$$

The N-point DFT and inverse DFT are defined in (5) and (6). A set of N-complex orthogonal time-domain elementary functions (complex sinewaves) now can be given as

$$\hat{x}_k(t) = \frac{1}{N} X(2\pi k/N)\, \mathrm{e}^{\mathrm{i}(2\pi k/N)t} \qquad k \in T^N \tag{18}$$

There holds

$$\sum_{k=0}^{N-1} \hat{x}_i(t)\hat{x}_j(t) = 0 \qquad \text{for } i \neq j$$

$$x(t) = \sum_{k=0}^{N-1} \hat{x}_k(t) \qquad \text{for } t \in T^N$$

Note that the elementary functions are also defined outside T^N, and that outside T^N they are given by periodic continuation. Hence, for $t \notin T^N$ the inverse N-point DFT gives a periodic continuation

$$x^R(t) = \sum_{k=0}^{N-1} \hat{x}_k(t) \qquad \text{for } t \in \mathbb{Z} \tag{19}$$

Consider the transformation matrix $W_N \in \mathbb{C}^{N \times N}$

$$W_N = \begin{bmatrix} 1 & 1 & \dots & 1 \\ 1 & e^{-j(2\pi/N)} & \dots & e^{-j(2\pi(N-1)/N)} \\ \vdots & \vdots & \ddots & \vdots \\ 1 & e^{-j(N-1)(2\pi/N)} & \dots & e^{-j(N-1)(2\pi(N-1)/N)} \end{bmatrix} \tag{20}$$

Note that $W_N/\sqrt{N}$ is an orthonormal matrix: $W_N W_N^*/N = W_N^* W_N/N = I$. W_N^* denotes the complex conjugate transpose of the matrix W_N. The N-point DFT can now be seen as a change of basis, where the new orthogonal set of basis functions is given by the columns of the matrix W_N. There holds

$$W_N \begin{bmatrix} \hat{x}_k(0) \\ \hat{x}_k(1) \\ \vdots \\ \hat{x}_k(N-1) \end{bmatrix} = \begin{bmatrix} 0 \\ \vdots \\ X(2\pi k/N) \\ \vdots \\ 0 \end{bmatrix} \tag{21}$$

where the nonzero element appears in the $(k+1)$th row. When a signal is used only over the time interval $T_{N_s}^N$, the DFT is defined according to (7), (8), and the elementary functions read

$$\begin{aligned} x(t) &= \sum_{k=0}^{N-1} \hat{x}_k^s(t) \qquad \text{for} \qquad t \in T_{N_s}^N \\ \hat{x}_k^s(t) &= \frac{1}{N} X^s(2\pi k/N)\, e^{j(2\pi k/N)(t-N_s)} \qquad \text{for} \qquad t \in T_{N_s}^N \end{aligned} \tag{22}$$

Finally, the past values of the input signal ($t < 0$) are sometimes denoted as $u^P(t)$ to stress that they are unknown.

A.2. Proof

The key observation is that we are able to decompose the input signal $u(t)$ over a measurement interval T^{N+N_s} in the basis W_N.

$$u(t) = \sum_{k=0}^{N-1} \hat{u}_k^s(t) \qquad \text{for } t \in T^{N+N_s}$$

This can be done only for partly periodic input signals, see (19). For $t \in T^{N+N_s}$ the output now can be written as

$$\begin{aligned} y(t) &= \sum_{i=0}^{\infty} g_0(i) u(t-i) + v(t) \\ &= \sum_{i=0}^{t} g_0(i) \sum_{k=0}^{N-1} \hat{u}_k^s(t-i) + \sum_{i=t+1}^{\infty} g_0(i) u^P(t-i) + v(t) \end{aligned} \tag{23}$$

Note that for an elementary function there holds

$$\begin{aligned} g_0(t) * \hat{u}_k^s(t) &= \sum_{i=0}^{\infty} g_0(i) \hat{u}_k^s(t-i) \\ &= \frac{1}{N} \sum_{i=0}^{\infty} g_0(i) U^s(2\pi k/N)\, e^{j(2\pi k/N)(t-N_s-i)} \\ &= \frac{1}{N} U^s(2\pi k/N)\, e^{j(2\pi k/N)(t-N_s)} \sum_{i=0}^{\infty} g_0(i)\, e^{-j(2\pi k/N)i} \\ &= \frac{1}{N} U^s(2\pi k/N)\, e^{j(2\pi k/N)(t-N_s)} G_0(2\pi k/N) \\ &= G_0(2\pi k/N) \hat{u}_k^s(t) \end{aligned} \tag{24}$$

where * denotes convolution. Hence

$$\sum_{i=0}^{t} g_0(i) \sum_{k=0}^{N-1} \hat{u}_k^s(t-i) = \sum_{k=0}^{N-1} \sum_{i=0}^{t} g_0(i)\hat{u}_k^s(t-i)$$
$$= \sum_{k=0}^{N-1} \left(\sum_{i=0}^{\infty} g_0(i)\hat{u}_k^s(t-i) - \sum_{i=t+1}^{\infty} g_0(i)\hat{u}_k^s(t-i) \right)$$
$$= \sum_{k=0}^{N-1} G_0(2\pi k/N)\hat{u}_k^s(t) - \sum_{i=t+1}^{\infty} g_0(i)u^R(t-i)$$

Equation (23) now can be written as

$$y(t) = \sum_{k=0}^{N-1} G_0(2\pi k/N)\hat{u}_k^s(t) + \sum_{i=t+1}^{\infty} g_0(i)\,[u^P(t-i) - u^R(t-i)] + v(t) \tag{25}$$

Define

$$e(t) = \sum_{i=t+1}^{\infty} g_0(i)\,[u^P(t-i) - u^R(t-i)] \tag{26}$$

Writing down equation (25) for all $t \in T_{N_s}^N$, and using equations (22) and (26) results in

$$\sum_{k=0}^{N-1} \begin{bmatrix} \hat{y}_k^s(N_s) \\ \hat{y}_k^s(N_s+1) \\ \vdots \\ \hat{y}_k^s(N_s+N-1) \end{bmatrix} = \sum_{k=0}^{N-1} G_0(2\pi k/N) \begin{bmatrix} \hat{u}_k^s(N_s) \\ \hat{u}_k^s(N_s+1) \\ \vdots \\ \hat{u}_k^s(N_s+N-1) \end{bmatrix}$$
$$+ \begin{bmatrix} e(N_s) \\ e(N_s+1) \\ \vdots \\ e(N_s+N-1) \end{bmatrix} + \begin{bmatrix} v(N_s) \\ v(N_s+1) \\ \vdots \\ v(N_s+N-1) \end{bmatrix} \tag{27}$$

Premultiplying with the $(l+1)$th row of W_N and using equation (21) gives

$$Y^s(2\pi l/N) = G_0(2\pi l/N)\,U^s(2\pi l/N) + E^s(2\pi l/N) + V^s(2\pi l/N)$$

By using the assumptions made on the impulse response and the input signal, an upper bound for $E^s(2\pi l/N)$ can be derived

$$|E^s(2\pi l/N)| \leqslant \left| \sum_{t=N_s}^{N_s+N-1} e^{-j(2\pi l/N)(t-N_s)} \sum_{i=t+1}^{\infty} g_0(i)\,[u^P(t-i) - u^R(t-i)] \right|$$
$$\leqslant (\bar{u}^p + \bar{u}) \sum_{t=N_s}^{N_s+N-1} \sum_{i=t+1}^{\infty} |g_0(i)|$$
$$\leqslant (\bar{u}^p + \bar{u}) \frac{M\rho}{(\rho-1)^2} \rho^{-N_s}(1-\rho^{-N}) \tag{28}$$

The result now follows by using the assumption made on the noise.

APPENDIX B: PROOF OF PROPOSITION 4.1

$$\left| \frac{d^k G_0(e^{j\omega})}{d\omega^k} \right| = \left| \frac{d^k}{d\omega^k} \left(\sum_{l=0}^{\infty} g_0(l)\, e^{-j\omega l} \right) \right| = \left| \sum_{l=0}^{\infty} g_0(l)(-jl)^k\, e^{-j\omega l} \right|$$
$$\leqslant \sum_{l=0}^{\infty} l^k |g_0(l)| \leqslant M \sum_{l=0}^{\infty} l^k \rho^{-k}$$

The use of standard Taylor series concludes the proof.

APPENDIX C: PROOF OF PROPOSITION 4.2

Write $F(e^{j\omega}) = G_0(e^{j\omega}) - G_{nom}(e^{j\omega})$. To prove the first inequality of Proposition 4.2 we now have to prove that for a scalar complex function $F(e^{j\omega})$ there holds

$$\left|\frac{d^k}{d\omega^k}|F(e^{j\omega})|\right| \leqslant \left|\frac{d^k F(e^{j\omega})}{d\omega^k}\right| \text{ for } k = \{1, 2\}$$

We will only give the proof for $k = 1$ (first derivative), the proof for $k = 2$ (second derivative) is completely analogous. Writing down the first derivative of $|F| = (F^*F)^{1/2}$ gives

$$\frac{d}{d\omega}|F| = \frac{1}{2|F|}\left(\frac{dF^*}{d\omega}F + F^*\frac{dF}{d\omega}\right)$$

Note that for any scalar complex function $F(e^{j\omega})$ there holds $d(F^*)/d\omega = (dF/d\omega)^*$ because

$$\lim_{\omega_2 \downarrow \omega_1} \frac{F^*(e^{j\omega_2}) - F^*(e^{j\omega_1})}{\omega_2 - \omega_1} = \lim_{\omega_2 \downarrow \omega_1}\left(\frac{F(e^{j\omega_2}) - F(e^{j\omega_1})}{\omega_2 - \omega_1}\right)^*$$

Therefore

$$\left|\frac{d}{d\omega}|F(e^{j\omega})|\right| \leqslant \frac{1}{2|F|}\left(|F|\left|\left(\frac{dF}{d\omega}\right)^*\right| + |F^*|\left|\frac{dF}{d\omega}\right|\right)$$

The first inequality of Proposition 4.2 now follows by noting that for any complex scalar a there holds $|a^*| = |a|$. The second inequality of Proposition 4.2 is just the triangle inequality.

APPENDIX D: INTERPOLATION ALGORITHM

To be able to give analytic expressions for the location of the maximum one has to distinguish several cases, depending on which part of the interpolating function $f(x)$ actually is used. It is, for example, possible that γ_1, γ_2, $\delta(\omega_k)$ and $\delta(\omega_{k+1})$ are such that the interpolating function $f(x)$ reduces to part I. In all, there are ten possibilities: only part I, only part II, part I and II, etc.

Algorithm D.1

All possibilities of the function given in equation (12) to interpolate two points are given below, as a function of Δx, Δy, γ_1 and γ_2.

A maximum occurs if

$$|\Delta y| < \gamma_1 \Delta x - \frac{\gamma_1^2}{2\gamma_2} \quad \text{and} \quad \Delta x \geqslant \frac{\gamma_1}{\gamma_2}$$

or if

$$|\Delta y| < \frac{\gamma_2}{2}\Delta x^2 \quad \text{and} \quad \Delta x \leqslant \frac{\gamma_1}{\gamma_2}$$

If a maximum occurs we can distinguish the following four cases.

1. If $\Delta x_1 \geqslant \gamma_1/\gamma_2$ and $\Delta x_2 \geqslant \gamma_1/\gamma_2$ then $\Delta x_1 = (\Delta y + \gamma_1 \Delta x)/(2\gamma_1)$.
   All four parts of $f(x)$, as depicted in Figure 1, are used.
2. If $\Delta x_1 \geqslant \gamma_1/\gamma_2$ and $\Delta x_2 < \gamma_1/\gamma_2$ then $\Delta x_1 = (\gamma_1/\gamma_2) + \Delta x - \sqrt{(2/\gamma_2)(\gamma_1 \Delta x - \Delta y)}$.
   Parts I, II and III of $f(x)$ are used.
3. If $\Delta x_1 < \gamma_1/\gamma_2$ and $\Delta x_2 \geqslant \gamma_1/\gamma_2$ then $\Delta x_1 = \sqrt{(2/\gamma_2)(\gamma_1 \Delta x + \Delta y)} - (\gamma_1/\gamma_2)$.
   Parts II, III and IV of $f(x)$ are used.
4. If $\Delta x_1 < \gamma_1/\gamma_2$ and $\Delta x_2 < \gamma_1/\gamma_2$ then $\Delta x_1 = (\Delta y/(\gamma_2 \Delta x)) + (\Delta x/2)$.
   Parts II and III of $f(x)$ are used.

The maximum height h_1 above $\delta(\omega_k)$ is given by $h_1 = -f(\Delta x_1)$, where $f(x)$ is given in equation (12).

If no maximum occurs we can distinguish the following six cases.

1. If $\gamma_1 \Delta x - (\gamma_2/2)\Delta x^2 \leqslant \Delta y < \gamma_1 \Delta x$ then $\Delta x_1 = (\gamma_1/\gamma_2) + \Delta x - \sqrt{(2/\gamma_2)(\gamma_1 \Delta x - \Delta y)}$.
   Note that $\Delta x_1 \geqslant \Delta x$. Parts I and II of $f(x)$ are used.

2. If $(\gamma_2/2)\,\Delta x^2 \leqslant \Delta y < \gamma_1\,\Delta x - (\gamma_2/2)\,\Delta x^2$ then $\Delta x_1 = (\Delta x/2) + (\Delta y/(\gamma_2\,\Delta x))$.
   Note that $\Delta x_1 \geqslant \Delta x$. Only part II of $f(x)$ is used.
3. If $\gamma_1\,\Delta x - (\gamma_2/2)\,\Delta x^2 \leqslant -\Delta y < \gamma_1\,\Delta x$ then $\Delta x_2 = (\gamma_1/\gamma_2) + \Delta x - \sqrt{(2/\gamma_2)(\gamma_1\,\Delta x + \Delta y)}$.
   Note that $\Delta x_2 \geqslant \Delta x$. Parts III and IV of $f(x)$ are used.
4. If $(\gamma_2/2)\,\Delta x^2 \leqslant -\Delta y < \gamma_1\,\Delta x - (\gamma_2/2)\,\Delta x^2$ then $\Delta x_2 = (\Delta x/2) - (\Delta y/(\gamma_2\,\Delta x))$.
   Note that $\Delta x_2 \geqslant \Delta x$. Only part III of $f(x)$ is used.
5. If $\Delta y = \gamma_1\,\Delta x$ then $\Delta x_1 = (\gamma_1/\gamma_2) + \Delta x$.
   Only part I of $f(x)$ is used.
6. If $\Delta y = -\gamma_1\,\Delta x$ then $\Delta x_2 = (\gamma_1/\gamma_2) + \Delta x$.
   Only part IV of $f(x)$ is used.

Proof. Direct computation. □

Using (12) and (13) an upper bound for the difference between the system and the nominal model over the whole frequency interval can be calculated.

REFERENCES

1. Bitmead, R. R., M. Gevers and V. Wertz, *Adaptive Optimal Control — Thinking Man's GPC*, Prentice Hall, Englewood Cliffs, NJ, 1990.
2. Bitmead, R. R., and Z. Zang, 'An iterative identification and control strategy', *Proc. European Control Conf.*, Grenoble, France, 2–5 July 1991, pp. 1396–1400.
3. Goodwin, G. C., and B. Ninness, 'Model error quantification for robust control based on quasi-bayesian estimation in closed loop', *Proc. American Control Conf.*, Boston, 26–28 June 1991, pp. 77–82.
4. Goodwin, G. C., and M. E. Salgado, 'Quantification of uncertainty in estimation using an embedding principle', *Proc. American Control Conf.*, Pittsburgh, 21–23 June 1989, pp. 1416–1421.
5. Gu, G., and P. P. Khargonekar, 'Linear and nonlinear algorithms for identification in H^∞ with error bounds', *Proc. American Control Conf.*, Boston, 26–28 June 1991, pp. 64–69.
6. Hakvoort, R. G., and R. J. P. Schrama, 'Approximate identification in view of LQG feedback design', *Proc. American Control Conf.*, Chicago, 24–26 June 1992, pp. 2824–2828.
7. Helmicki, A. J., C. A. Jacobson and C. N. Nett, 'Identification in H_∞: a robustly convergent, nonlinear algorithm', *Proc. American Control Conf.*, San Diego, 23–25 May 1990, pp. 386–391.
8. Helmicki, A. J., C. A. Jacobson and C. N. Nett, 'Identification in H_∞: linear algorithms', *Proc. American Control Conf.*, San Diego, 23–25 May 1990, pp. 2418–2423.
9. Kosut, R. L., M. Lau and S. Boyd, 'Identification of systems with parametric and nonparametric uncertainty', *Proc. American Control Conf.*, San Diego, 23–25 May 1990, pp. 2412–2417.
10. LaMaire, R. O., L. Valavani, M. Athans and G. Stein, 'A frequency-domain estimator for use in adaptive control systems', *Automatica*, **27**, 23–38 (1991).
11. Ljung, L., *System Identification: Theory for the User*, Prentice Hall, Englewood Cliffs, NJ, 1987.
12. Schoukens, J., P. Guillaume and R. Pintelon, 'Design of multisine excitations', *IEE Control 91 Conference*, Edinburgh, 25–28 March 1991.
13. Schrama, R. J. P., 'Control-oriented approximate closed-loop identification via fractional representations', *Proc. American Control Conf.*, Boston, 26–28 June 1991, pp. 719–720.
14. Schrama, R. J. P., and P. M. J. Van den Hof, 'An iterative scheme for identification and control design based on coprime factorizations', *Proc. American Control Conf.*, Chicago, 24–26 June 1992, pp. 2842–2846.
15. Wahlberg, B., and L. Ljung, 'On estimation of transfer function error bounds', *Proc. European Control Conf.*, Grenoble, France, 2–5 July 1991, pp. 1378–1383.